available at www.sciencedirect.com

ScienceDirect

journal homepage: www.elsevier.com/locate/ijggc

Predicting PVT data for CO_2–brine mixtures for black-oil simulation of CO_2 geological storage

Hassan Hassanzadeh [a], *Mehran Pooladi-Darvish* [a,*], *Adel M. Elsharkawy* [b], *David W. Keith* [a], *Yuri Leonenko* [a]

[a] *Department of Chemical and Petroleum Engineering, University of Calgary, Canada*
[b] *Department of Petroleum Engineering, Kuwait University, Kuwait*

ARTICLE INFO

Article history:
Received 15 September 2006
Received in revised form
20 December 2006
Accepted 21 December 2006
Published on line 9 February 2007

Keywords:
Black-oil flow simulation
Compositional simulation
CO_2 storage or sequestration
PVT data

ABSTRACT

Accurate modeling of the storage or sequestration of CO_2 injected into subsurface formations requires an accurate fluid model. This can be achieved using compositional reservoir simulations. However, sophisticated equations of state (EOS) approaches used in current compositional simulators are computationally expensive. It is advantageous and possible to use a simple, but accurate fluid model for the very specific case of geological CO_2 storage. Using a black-oil simulation approach, the computational burden of flow simulation can be reduced significantly. In this work, an efficient and simple algorithm is developed for converting compositional data from EOS into black-oil PVT data. Our algorithm is capable of predicting CO_2–brine density, solubility, and formation volume factor, which are all necessary for black-oil flow simulations of CO_2 storage in geological formations. Numerical simulations for a simple CO_2 storage case demonstrate that the black-oil simulation runs are at least four times faster than the compositional ones without loss of accuracy. The accuracy in prediction of CO_2–brine black-oil PVT properties and higher computational efficiency of the black-oil approach promote application of black-oil simulation for large-scale geological storage of CO_2 in saline aquifers.

1. Introduction

The sequestration of anthropogenic CO_2 into geological formations has been considered as a potential method to mitigate climate change. Accurate evaluation of the capacity of a saline aquifer for CO_2 sequestration, and the fate of the injected fluids in sedimentary basins needs precise representation of brine and CO_2 PVT data (Adams and Bachu, 2002; Bachu and Adams, 2003). Experimental data reported in the literature show that the density of an aqueous solution of CO_2 could be slightly greater than that of pure water (Blair and Quinn, 1968; Sayegh and Najman, 1987; Hnedovsky et al., 1996). This density variation might cause free convection motion, which in turn causes increased dissolution over a larger distance and shorter time scales compared to pure diffusive flow (Lindeberg and Wessel-Berg, 1996; Ennis-King and Paterson, 2003, 2005; Ennis-King et al., 2005; Hassanzadeh et al., 2005). Therefore, accurate description of the thermodynamic and transport properties of CO_2 and brine are very important for evaluating the capacity of saline aquifers to sequester CO_2 by a solubility trapping mechanism.

In the petroleum industry, compositional reservoir simulators use EOS thermodynamic models to calculate the phase equilibrium properties of fluid mixtures (Chang et al., 1998). Although these kinds of thermodynamic models are well suited for compositional modeling of enhanced oil recovery

* *Corresponding author*. Tel.: +403 220 8779; fax: +403 284 4852.
E-mail address: pooladi@ucalgary.ca (M. Pooladi-Darvish).
1750-5836/$ – see front matter
doi:10.1016/S1750-5836(07)00010-2

Nomenclature

a	equation of state parameter
a	activity
b	equation of state parameter
B_b	brine formation volume factor
c_b	formation brine compressibility
D	molecular diffusion coefficient
k	constant = 1.38058×10^{-12}
K	equilibrium ratio
m	molality
M_w	molecular weight
n	mole
p	pressure
Par	parameter, it can be either λ or ζ
R	gas constant
R_s	dissolved CO_2–brine ratio
T	absolute temperature (K)
V	volume
$\bar{V}$	molar volume
V_ϕ	apparent molar volume
x	mole fraction in aqueous phase
y	mole fraction in CO_2-rich phase
Z	CO_2 compressibility factor

Greek symbols

γ	activity coefficient
φ	fugacity coefficient
κ	equilibrium constant
λ	second-order interaction parameters
μ	viscosity
ν	stoichiometric number of ions in the dissolved salt
π	pressure
θ	temperature (°C)
ρ	mass density
$\bar{\rho}$	molar density
ω	CO_2 mass fraction in aqueous phase
ζ	third-order interaction parameters

Subscripts

A	anion
b	brine
C	cation
i	component index
j	component index
k	component index
L	liquid
m	mixture
res	Reservoir condition
sat	saturated
sc	standard condition
w	water
1	solvent
2	solute

Superscript

°	reference state

(EOR) processes, such as miscible gas injection, the disadvantage of such models for the specific case of large-scale flow simulation of geological CO_2 storage in aquifers is that they represent computational ''overkill'' and are inappropriately expensive. Therefore, it would be helpful if we were able to use a simple thermodynamic model that can predict the CO_2–brine equilibrium properties accurately with less computational overhead. Indeed, there are a large number of experimental equilibrium data on the CO_2–brine system that have been used to develop correlations and tune the equations of state for CO_2 and water under subsurface conditions. Such experimental and EOS data are used in this paper to develop a black-oil PVT module needed for flow simulation geological storage of CO_2 in saline aquifers. The novelty of this work is in presenting a PVT module for converting compositional data into black-oil that provides accurate PVT data required for black-oil flow simulation of CO_2 storage in saline aquifers. The black-oil PVT module developed in this work is validated with experimental data available in the literature. Furthermore, our numerical flow simulations of CO_2 storage reveal that the black-oil simulation approach is computationally more efficient than the compositional approach. The accuracy in prediction of CO_2–brine PVT properties and superior computational efficiency encourages application of black-oil simulation approach for large-scale geological storage of CO_2 in saline aquifers.

The thermodynamic model used in this work is based on a combination of the Duan and Sun (2003) and Spycher et al. (2003) models. Similar models have recently appeared in the literature (Spycher and Pruess, 2005; Portier and Rochelle, 2005; Duan et al., 2006). In this paper, in addition to presentation of our thermodynamic module, we use it to generate CO_2–brine PVT properties as required for black-oil flow simulation. For completeness, we also present the correlations of transport properties of the CO_2 and brine system required for black-oil reservoir simulation.

This paper is organized as follows. First a brief review of the literature on thermodynamic modeling of CO_2–brine equilibrium is presented. Then, the thermodynamic model used in this study is described and its results are compared with experimental data available in the literature. This is followed by the main contribution of the paper; representation of the CO_2–brine PVT properties suitable for black-oil simulation and a comparison of black-oil and compositional simulator computational performances for simulation of CO_2 injection into saline aquifers.

2. Review of CO_2–brine solubility data

The CO_2–water equilibrium phenomenon has been studied extensively in literature. The interested reader might consult more exhaustive reviews from Diamond and Akinfiev (2003), Duan and Sun (2003), and Spycher et al. (2003) among others. In this section, a brief review of some of the studies is presented. Wiebe and Gaddy (1939) and Wiebe (1941) reported experimental solubility of CO_2 in water at temperatures up to 100 °C and pressures up to 700 atm. Dodds et al. (1956) have used available equilibrium data on the solubility of carbon dioxide in water to develop a chart for determination of CO_2

solubility in water as a function of pressure and temperature. Their work covers a temperature range of 0–120 °C and a pressure range of 1–700 atm. Rowe and Chou (1970) have measured thermodynamic properties of NaCl solutions in the temperature range of 0–175 °C for NaCl concentrations of 0–25 g per 100 g of solution and pressures up to 34 MPa. They developed a correlation, which describes the PVT–x relation to fit their experimental data as well as the density data from the literature. Enick and Klara (1990) have used 110 solubility data from the literature for the CO_2–water system over a temperature range of 298–523 K and a pressure range of 3.40–72.41 MPa to determine the reference Henry's constant. They developed an empirical correlation that can be used to calculate the reference Henry's constant for the CO_2–water system. Span and Wagner (1996) reviewed the available data on thermodynamic properties of CO_2 and presented a new equation of state in the form of a fundamental equation explicit in the Helmholtz free energy that accurately represents the experimental data. Battistelli et al. (1997) developed an equation of state module for the TOUGH2 simulator for water, salt, and gas suitable for geothermal reservoir modeling. Their Henry's constant correlation for water and CO_2 was based on experimental data using a polynomial regression for a temperature range of 0–300 °C and salinity up to 4.87 molal. Teng et al. (1997) presented an experimental investigation on the solubility of CO_2 as a liquid in water at temperatures from 278 to 293 K and pressures from 6.44 to 29.49 MPa. They presented an expression for Henry's constant as a function of pressure and temperature based on experimental data. They also developed an expression relating the density of CO_2 aqueous solution and pure water. Garcia (2001) presented a correlation for calculation of partial molar volume of CO_2 in water. He reported a density increase of 2–3% for an aqueous solution of CO_2 in water compared to pure water. An excellent work by Spycher et al. (2003) reviewed the published experimental P–T–x data in the temperature range of 12–100 °C and pressure up to 600 bar to develop a solubility model. They used a non-iterative procedure to calculate the composition of the compressed CO_2 and liquid phase at equilibrium based on equating chemical potentials and using the Redlich–Kwong equation of state without accounting for salinity. Their procedure avoids iteration and is suitable for computationally intensive flow simulation. Duan and Sun (2003) presented an improved and highly accurate model for calculation of CO_2 solubility in pure water and NaCl aqueous solutions from 273 to 533 K and pressures up to 2000 bar. Their model is based on particle interaction theory for the liquid phase and an equation of state for the vapor phase. Diamond and Akinfiev (2003) used published solubility data in the literature to evaluate the solubility of CO_2 in water. They found that the assumption that the activity coefficients of aqueous CO_2 are equal to unity is valid up to solubilities of approximately 2 mol%. Wong et al. (2005) used available thermodynamic data for liquid CO_2 and CO_2 gas solubility in seawater and developed an equation for the solubility of liquid CO_2 in seawater as a function of temperature, pressure, and salinity.

In the following, the thermodynamic model used in developing a PVT module for predicting black-oil data required for flow simulation of geological CO_2 storage in saline aquifers is presented.

3. Thermodynamic model

From the definition of fugacity, we have:

$$f_i = \varphi_i y_i p \tag{1}$$

where f denotes fugacity; φ fugacity coefficient; p total pressure; y is the mole fraction in the gaseous phase. At equilibrium, the following equilibrium relationship holds (Spycher et al., 2003):

$$\kappa_{H_2O} = \frac{f_{H_2O(g)}}{a_{H_2O(aq)}} \tag{2}$$

$$\kappa_{CO_2} = \frac{f_{CO_2(g)}}{a_{CO_2(aq)}} \tag{3}$$

where κ parameters are true equilibrium constants and a is the activity of a component in the aqueous phase. The κ parameters are functions of pressure and temperature as given by the following expression (Spycher et al., 2003):

$$\kappa(T, p) = \kappa^0_{(T,p^0)} \exp\left[\frac{(p - p^0)\bar{V}_i}{RT}\right] \tag{4}$$

where the exponential term is termed the Poynting factor; p pressure; p^0 reference pressure (1 bar); T temperature in K; R gas constant; $\bar{V}_i$ is the average partial molar volume of the pure condensed component i over the pressure interval p^0 to p and it is assumed constant in the pressure interval of interest (Spycher et al., 2003).

Substituting for fugacities in Eq. (1) from Eqs. (2) and (3) gives:

$$f_{H_2O} = \varphi_{H_2O} y_{H_2O} p = \kappa_{H_2O} a_{H_2O(a)} \tag{5}$$

$$f_{CO_2} = \varphi_{CO_2} y_{CO_2} p = \kappa_{CO_2(g)} a_{CO_2(aq)} \tag{6}$$

Then, substituting for $\kappa(T, p)$ results in:

$$y_{H_2O} = \frac{\kappa^0_{H_2O} a_{H_2O}}{\varphi_{H_2O} p} \exp\left[\frac{(p - p^0)\bar{V}_{H_2O}}{RT}\right] \tag{7}$$

The activity of the water component can be approximated by its mole fraction $a_{H_2O} = 1 - x_{CO_2} - x_{salt}$, where x_{CO_2} and x_{salt} are CO_2 and salt mole fractions, respectively.

In the petroleum industry, the salinity of the formation brine is generally reported as a constant in terms of total dissolved solids (water/NaCl solution of equivalent total dissolved solid) (Amyx et al., 1960; Craft et al., 1991; Enick and Klara, 1992; Walsh and Lake, 2003, among others). In other words, the effect of different salts is simply accounted through lumping of all dissolved salts into their salinity equivalent. However, Spycher and Pruess (2005) treated x_{salt} as a variable in their model to include the variation in salt concentration in equilibrium calculation. Calculations based on the Spycher and Pruess (2005) model reveal that x_{salt} is fairly constant for the pressure and temperature range of CO_2 storage in saline aquifers. This is due to the fact that CO_2 solubility in aqueous phase is very low. Therefore, for the purpose of generating

black-oil PVT data, we assumed that x_{salt} is constant in our calculations.

Similarly, using $a_{CO_2} = 55.508\gamma_{CO_2}x_{CO_2}$, where γ_{CO_2} is the activity coefficient of the dissolved CO_2, results in (Spycher et al., 2003):

$$\frac{y_{CO_2}}{x_{CO_2}} = \frac{55.508\kappa^0_{CO_2(g)}\gamma_{CO_2}}{\varphi_{CO_2}p}\exp\left[\frac{(p-p^0)\bar{V}_{CO_2}}{RT}\right] \quad (8)$$

where $\bar{V}_{H_2O} = 18.1\ cm^3/mol$, $\bar{V}_{CO_2(g)} = 32.6\ cm^3/mol$, $\bar{V}_{CO_2(l)} = 32\ cm^3/mol$, and the κ parameters for CO_2 and water are given by (Spycher et al., 2003):

$$\log\kappa^0_{CO_2(g)} = 1.189 + 1.304\times10^{-2}\theta - 5.446\times10^{-5}\theta^2 \quad (9)$$

$$\log\kappa^0_{CO_2(l)} = 1.169 + 1.368\times10^{-2}\theta - 5.380\times10^{-5}\theta^2 \quad (10)$$

$$\log\kappa^0_{H_2O} = -2.209 + 3.097\times10^{-2}\theta - 1.098\times10^{-4}\theta^2 + 2.048\times10^{-7}\theta^3 \quad (11)$$

where θ is temperature in °C.

Here we have applied the approach used by Spycher et al. (2003) to calculate component fugacities in the CO_2-rich phase by using the Redlich and Kwong (1949) equations of state (EOS) and the Duan and Sun (2003) model to calculate the activity coefficient of CO_2. See Appendix A for details on RK equations of state. The fugacity of each component in the CO_2-rich phase depends on the phase composition. Therefore, the above computations should be performed iteratively. However, the water mole fraction in the CO_2-rich phase is very small and can be neglected in calculation of the mixing rules as suggested by Spycher et al. (2003), which in turn avoids iteration.

To calculate the CO_2 activity coefficient, the virial expansion of Gibbs excess energy (Pitzer, 1973) is used, as given by Duan and Sun (2003) in the following expression:

$$\ln\gamma^*_{CO_2} = \sum_C 2m_C\lambda_{CO_2-C} + \sum_A 2m_A\lambda_{CO_2-A} + \sum_C\sum_A m_C m_A\zeta_{CO_2-A-C} \quad (12)$$

with $\gamma^*_{CO_2} = m^0_{CO_2}/m_{CO_2}$, where $m^0_{CO_2}$ and m_{CO_2} are the CO_2 molality in pure and saline water, respectively as recently identified by Spycher and Pruess (2005). The parameters λ_{CO_2-C} and ζ_{CO_2-A-C} are second- and third-order interaction parameters, respectively, and $\lambda_{CO_2-A} = 0$ as suggested by Duan and Sun (2003). The subscripts A and C denote anions and cations, respectively. Parameters λ and ζ are dependent on temperature and total pressure. In this work, the following parametric equation is used to calculate λ and ζ, after Duan and Sun (2003):

$$\mathrm{Par}(T,p) = c_1 + c_2T + \frac{c_3}{T} + \frac{c_4p}{T} + \frac{c_5p}{630-T} + c_6T\ln p \quad (13)$$

where Par(T, p) can be either λ or ζ, T is temperature in K and p is pressure in bar. Table 1 gives the constants needed to calculate the interaction parameters.

Table 1 – Constants needed to evaluate the interaction parameters in Eq. (12) (from Duan and Sun, 2003)

Coefficient	λ_{CO_2-Na}	$\zeta_{CO_2-Na-Cl}$
c_1	−0.411370585	3.36389723×10^{-4}
c_2	6.07632013×10^{-2}	-1.98298980×10^{-2}
c_3	97.5347708	0
c_4	−0.0237622469	2.122220830×10^{-3}
c_5	0.0170656236	-5.24873303×10^{-3}
c_6	1.41335834×10^{-5}	0

The molality of CO_2 in pure water can be calculated by setting $x_{salt} = 0$ in Eqs. (7) and (8) and $m^0_{CO_2} = 55.508x_{CO_2}/x_{H_2O}$ as outlined in Appendix B. The molality of CO_2 in saline water is then calculated with $m_{CO_2} = m^0_{CO_2}/\gamma_{CO_2}$. Using the molality of CO_2 in saline water, the mole fraction of CO_2 in the aqueous phase can be obtained from the following expression (Spycher and Pruess, 2005):

$$x_{CO_2} = \frac{m_{CO_2}}{m_{CO_2} + 55.508 + \nu m_s} \quad (14)$$

where m_s is salt molality and ν is the stoichiometric number of ions in the dissolved salt.

Component mole fractions and equilibrium ratios can be obtained by the following equations:

$$x_{H_2O} = 1 - x_{CO_2} - x_{salt} \quad (15)$$

$$y_{H_2O} = \frac{\kappa^0_{H_2O}(1-x_{CO_2}-x_{salt})}{\varphi_{H_2O}p}\exp\left[\frac{(p-p^0)\bar{V}_{H_2O}}{RT}\right] \quad (16)$$

$$y_{CO_2} = 1 - y_{H_2O} \quad (17)$$

$$K_{CO_2} = \frac{y_{CO_2}}{x_{CO_2}} \quad (18)$$

$$K_{H_2O} = \frac{y_{H_2O}}{x_{H_2O}} \quad (19)$$

A detailed procedure for the calculation of compositional data into black-oil PVT data is presented in Appendix B.

The CO_2 saturated aqueous phase density is obtained using the approach of Garcia (2001) as given by

$$\rho_{sat} = \frac{1 + (M_{w_2}/M_{w_1})(x_2/x_1)}{(V_\phi/M_{w_1})(x_2/x_1) + (1/\rho_1)} \quad (20)$$

where ρ_{sat} is in kg/m^3, and ρ_1 and ρ_2 are solvent and solute densities in kg/m^3, respectively. The partial molar volume is calculated by

$$V_\phi = 37.51 - 9.585\times10^{-2}\theta + 8.740\times10^{-4}\theta^2 - 5.044\times10^{-7}\theta^3 \quad (21)$$

where V_ϕ is in cm^3/mol.

Using the above formulation, CO_2 and water composition in both phases can be obtained. The combined formulation above is used to calculate the equilibrium ratios and to generate black-oil PVT data for a CO_2–water mixture as detailed in Appendix B. In the following section a comparison with the experimental data in the literature is presented.

4. Comparison with experimental data

Chang et al. (1998), Diamond and Akinfiev (2003), Duan and Sun (2003), Spycher et al. (2003), Spycher and Pruess (2005), Portier and Rochelle (2005), and Duan et al. (2006) reviewed and used CO_2–brine mixture data available in the literature to develop their solubility model. In this section, we compare the calculated CO_2–water properties with such experimental data from the literature. These experimental data are taken from King et al. (1992), Wiebe and Gaddy (1939, 1940), Wiebe (1941), Malinin and Savelyeva (1972), Malinin and Kurovskaya (1975), Song and Kobayashi (1987), Tödheide and Frank (1963), Müller et al. (1988), Gillespie and Wilson (1982), Sako et al. (1991), Dohrn et al. (1993), Briones et al. (1987), D'Souza et al. (1988), and Bamberger et al. (2000). In each case, the thermodynamic module of this work is used to calculate the properties as shown in their original units reported in the references.

Fig. 1 shows a comparison between predicted equilibrium ratios and those from experimental data available in the literature. The comparison demonstrates an acceptable match in the temperature range of 25–80 °C and a pressure range of 0–100 MPa.

A comparison between solubility of CO_2 in the aqueous phase calculated using the proposed module versus the experimental data reported by Wiebe (1941) is presented in Fig. 2. Results presented in Fig. 2 show a good agreement between experimental data and that predicted by the module for the pressure range typically encountered in geological CO_2 storage. Fig. 3 shows the effect of salinity on the dissolution of CO_2 in saline water. The results calculated are validated with the experimental data reported by Malinin and Savelyeva (1972) and Malinin and Kurovskaya (1975). This figure indicates that the model successfully predicts the CO_2–brine solubility as a function of salinity and is able to match the experimentally measured solubility.

Fig. 4(a) shows a comparison of the mole fraction of CO_2 in the aqueous phase predicted by the model versus the experimental data reported by Wiebe (1941). The vapor phase mole fraction of the water component is shown in Fig. 4(b). The module predictions of mole fractions are in close agreement with the experimental data of Wiebe (1941) at various temperatures and pressures. An extensive comparison of the results obtained using this study with other predictive tools is presented by Hassanzadeh (2006). It was found that the predictions of the proposed module are at least comparable to those reported elsewhere. We also compared CO_2 density in the supercritical region (not shown here) with those reported by Span and Wagner (1996) and found an acceptable agreement. In the following, the thermodynamic calculations are used to generate PVT properties as required in black-oil flow simulation.

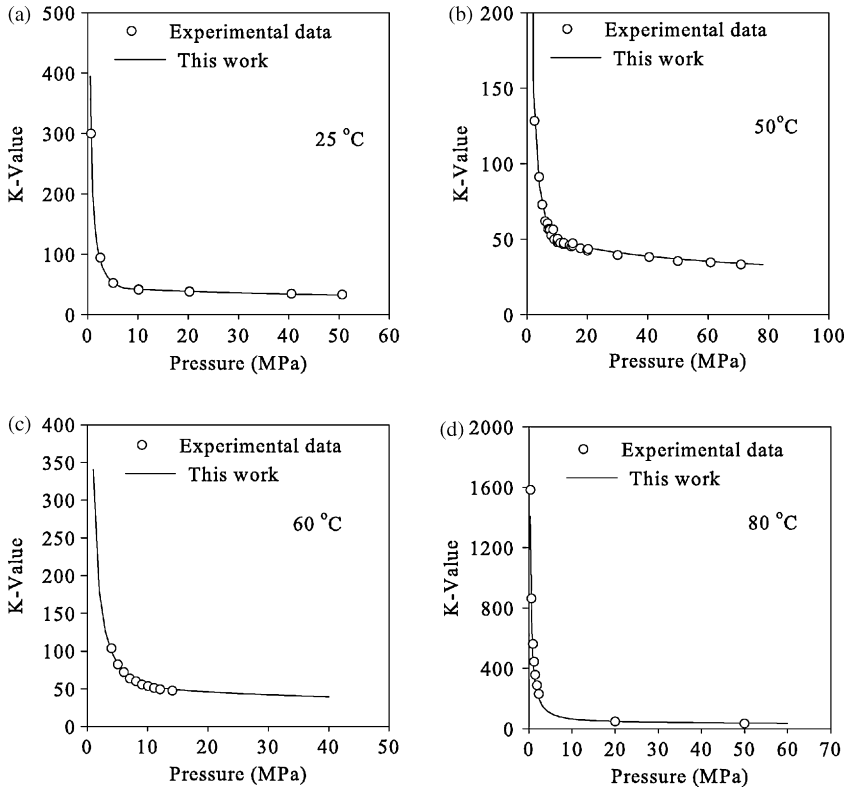

Fig. 1 – Comparison between experimental data and calculated equilibrium ratio by the proposed module for a CO_2–water mixture for various temperatures: (a) 25 °C; (b) 50 °C; (c) 60 °C; (d) 80 °C. The experimental data are taken from Wiebe and Gaddy (1939), Wiebe and Gaddy (1940), Wiebe (1941), Song and Kobayashi (1987), Tödheide and Frank (1963), Müller et al. (1988), Gillespie and Wilson (1982), Briones et al. (1987), D'Souza et al. (1988), Sako et al. (1991), King et al. (1992), Dohrn et al. (1993), and Bamberger et al. (2000).

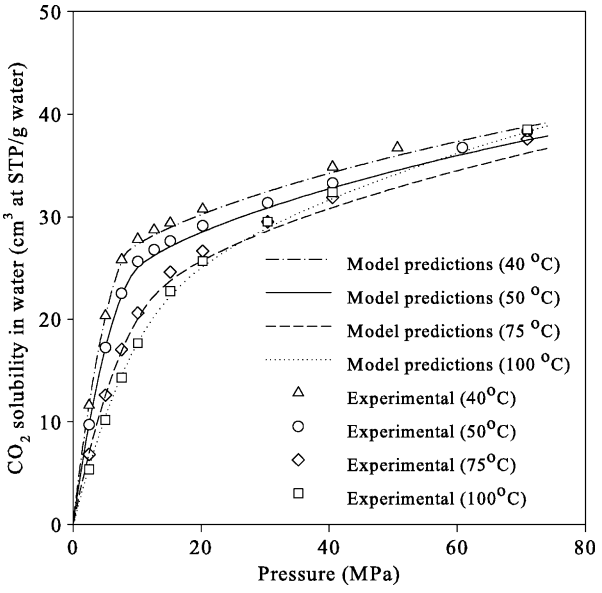

Fig. 2 – Solubility of CO_2 in water calculated by proposed module and the experimental data of Wiebe (1941) as a function of pressure.

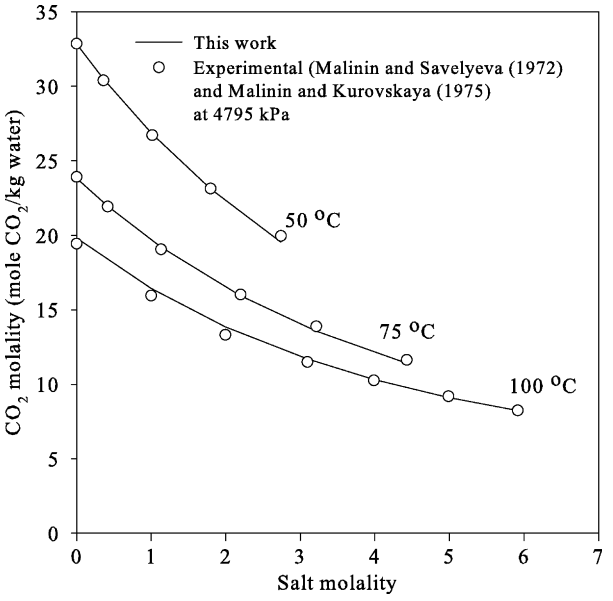

Fig. 3 – Predicted CO_2 solubility at 4795 kPa in brines of different salinity at various temperatures versus the experimental data of Malinin and Savelyeva (1972) and Malinin and Kurovskaya (1975).

5. Representation of CO_2–brine equations of state predictions in a black-oil simulator

The choice of the fluid model is very important in any flow simulation including simulation of CO_2 storage in saline aquifers. Black-oil flow simulators have been used for modeling fluid flow in petroleum reservoirs, when the reservoir fluids can be lumped into three components, oil, gas and water (Aziz and Settari, 1979). In such simulators, these three components can be partitioned in three phases generically called oil, gas and water. In this system, the gas component is usually partitioned between the oil and gas phases, while the oil and water components generally exist only in oil and water phases, respectively. On the other hand, compositional models have been developed to simulate more complex phase equilibrium systems such as those in miscible gas injection, when partitioning of a larger number of components is important.

In an iso-thermal multi-component system, partitioning of each component depends on pressure and composition. However, when using black-oil formulation for a CO_2–brine system, accurate PVT calculations can be achieved using standard black-oil PVT tables as a function of pressure only. Therefore, the phase equilibrium calculations in black-oil models are very fast and simplified by table look-up of black-oil input data. This leads to much less computational time as compared to time-consuming compositional calculations that require frequent equations of state phase equilibrium calculations. Computation times using black-oil and compositional simulation for a CO_2 injection study are compared in the next section.

The implementation of the fluid module presented in this work is very simple. The input data for the fluid module are temperature and salinity. Having these two data points, the module will provide black-oil PVT data needed for black-oil flow simulation such as formation volume factor, solubility, viscosity and compressibility factor as a function of pressure. As mentioned, in contrast to multi-component hydrocarbon systems, we are dealing with two components only; CO_2 and brine. There is a large number of experimental data available in the literature that has been used to tune the equations of state for the CO_2–brine mixture. Therefore, no experimental measurements are needed and an accurate prediction of thermodynamic data is possible using the developed module.

Two main parameters in black-oil simulators are solution gas-oil ratio and oil formation volume factor. In order to use a black-oil simulator for CO_2 storage simulation, one needs to represent the brine and CO_2 by oil and gas, respectively. The solution gas–oil ratio (CO_2–brine ratio) and the oil (brine) formation volume factor are defined as

$$R_s = \frac{V_{d\,CO_2 sc}}{V_{b\,sc}} \tag{22}$$

$$B_b = \frac{V_{d\,CO_2 res} + V_{b\,res}}{V_{b\,sc}} \tag{23}$$

where $V_{d\,CO_2 sc}$ and $V_{d\,CO_2 res}$ are the volume of dissolved CO_2 in formation brine at standard and reservoir conditions, respectively, and $V_{b\,sc}$ and $V_{b\,res}$ are the formation brine volume at standard and reservoir conditions, respectively. The parameters in Eqs. (22) and (23) can be expressed in terms of the equilibrium properties of the CO_2–brine mixture obtained from a tuned equation of state. The CO_2 solubility in brine can be represented by the solution gas–oil ratio function as presented by

$$R_s = \frac{\bar{\rho}_{b\,sc} x_{CO_2}}{\bar{\rho}_{CO_2 sc}(1 - x_{CO_2})} \tag{24}$$

where $\bar{\rho}_{b\,sc}$ and $\bar{\rho}_{CO_2 sc}$ are the formation brine and CO_2 molar density at standard conditions, and x_{CO_2} is the CO_2 mole

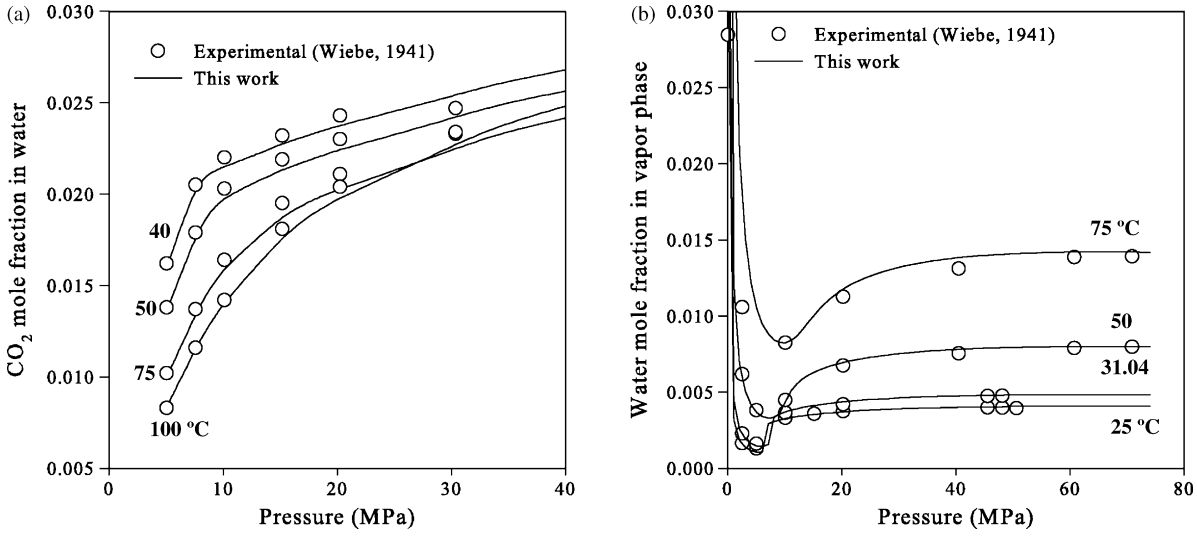

Fig. 4 – Mole fraction of CO_2 in the aqueous phase (a) and water mole fraction in the vapor phase (b) as a function of pressure at various temperatures versus the experimental data of Wiebe (1941).

fraction in aqueous phase. In addition, the shrinkage and swelling of the brine due to CO_2 release and dissolution can be represented by the oil formation volume factor in a black-oil simulator as given by

$$B_b = \frac{\rho_{b\,sc}}{\rho_{b\,res}(1-\omega_{CO_2})} \tag{25}$$

where $\rho_{b\,sc}$ and $\rho_{b\,res}$ are the formation brine mass density at standard and at reservoir conditions, respectively, and ω_{CO_2} is the CO_2 mass fraction in aqueous phase. Therefore, the PVT data include gas–oil ratio (R_s) and formation volume factor (B_b) as a function of pressure. Water and CO_2 viscosity (μ_b, μ_g), brine compressibility (c_b), and the gas compressibility factor (Z) are also needed as input data. The gas compressibility factor (Z) may be calculated using the Redlich and Kwong EOS (1949). The brine compressibility and density are calculated using the Rowe and Chou (1970) correlation. Brine and CO_2 viscosities as functions of pressure, temperature, and salinity are calculated using the Kestin et al. (1981), Vesovic et al. (1990), and Fenghour et al. (1998) correlations, respectively. The molecular diffusion coefficient of CO_2 into brine is also calculated using available correlations in the literature (Ratcliff and Holdcroft, 1963; McLachlan and Danckwerts, 1972; Al-Rawajfeh, 2004). It is noted that the molecular diffusion may not be important in black-oil simulations for flow simulations for oil and gas reservoirs. However, in CO_2 storage in deep saline aquifers we are dealing with century-long time scales where the molecular diffusion becomes important (Lindeberg and Wessel-Berg, 1996). Therefore, for completeness we included a well-known correlation for calculation of molecular diffusion coefficient. A summary of the correlations for transport properties of CO_2 and brine are presented in Appendix C. A sample of generated PVT data is presented in Fig. 5. These data are used in the following section, where a comparison of the black-oil and compositional computational efficiency is presented.

6. Performance comparison of black-oil and compositional simulations

Compositional reservoir simulators are well known to be more time consuming than black-oil simulators. This is due to the fact that compositional simulators perform frequent phase equilibrium and flash calculations at each time step. Furthermore, the formulation in compositional simulators is more complicated. Very often, this results in a larger number of time-steps used by the compositional simulator. Compositional simulators may have stability limitations resulting from the time approximation of phase transmissibilities, the approximation of new composition, and the iterative solution of the phase equilibrium calculations (Settari, 2001). On the other hand, black-oil reservoir simulators have the benefit of a simpler numerical formulation and lower stability limitations and, therefore, perform faster than compositional simulators because of smaller number of calculations per time-step and smaller number of time-steps.

The CO_2–brine displacement in porous media is a difficult numerical problem due to adverse mobility ratio and gravitational segregation (Aziz and Settari, 1979). In addition, the phase equilibrium calculation of CO_2–brine is also computationally more difficult for current reservoir simulation technology. In the following, we have shown that the work per time step for a black-oil simulator is smaller than that of a compositional simulator for CO_2 storage in saline aquifers, and that the stability criterion of the compositional simulator results in smaller time-steps as compared with the black-oil simulator.

Black-oil and compositional simulations of CO_2 storage into a saline aquifer are presented. The run times have been compared for these two approaches for the simulation of CO_2 into deep saline aquifers. Black-oil (IMEX, 2004) and compositional (GEM, 2004) options from a commercial reservoir simulator (CMG) are used to perform the numerical simulations. A simple two-dimensional radial problem addresses the two-phase flow of CO_2 and 150,000 ppm saline water under

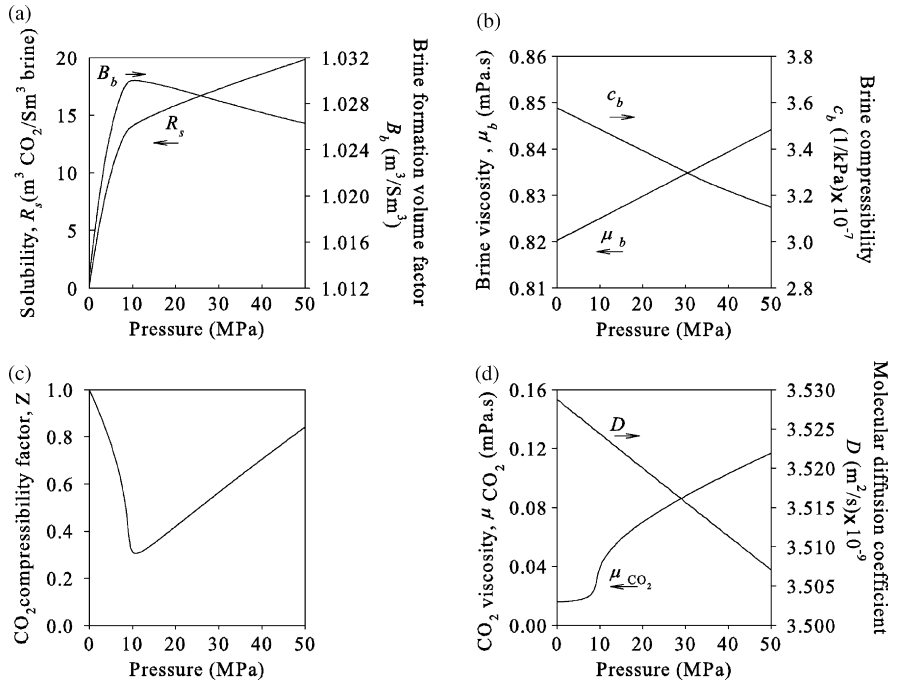

Fig. 5 – CO_2 and brine PVT data as functions of pressure for 150,000 ppm salinity at 50 °C needed for using a black-oil flow simulator. (a) CO_2 solubility and brine formation volume factor; (b) brine compressibility and viscosity; (c) CO_2 compressibility factor; (d) CO_2 viscosity and molecular diffusion coefficient of CO_2 in brine.

isothermal condition of 45 °C. The aquifer with a thickness of 100 m and the radius of 100 km is assumed homogeneous and isotopic with permeability of 200 mD, porosity of 0.25 and rock compressibility of 1.45×10^{-7} 1/kPa. The numerical model consists of 90 grid blocks in the radial direction and 80 grid blocks in the vertical direction. The relative permeability curves for CO_2 and brine are calculated using the Corey function (Honarpour et al., 1982). The aquifer is initially saturated with brine and the pressure at top of the aquifer is 12 MPa.

Carbon dioxide is injected at a rate of 1 Mt/year during the first 30 years of simulation into the aquifer. All the conditions and parameters described above remained the same for both black-oil and compositional simulations. Both simulators provided very close results for pressure, water and gas saturation distributions and well bottom pressure. The difference in pressure field (including well pressure) during the simulation is less than 0.3%. For the saturation distributions the difference in results is less than 3%.

Commercial simulators have an automatic time-step selection module that allows selection of larger time-steps unless accuracy or stability is compromised. In the simulation studies performed here, it was found that the black-oil simulator chooses larger time-steps than the compositional simulator. In order to compare the amount of CPU time for similar time-steps, the maximum allowable time-step was controlled. Fig. 6 shows the CPU times for both simulators when two different maximum time-steps of 1 and 10 days were used. In the first case (maximum time step of 1 day),

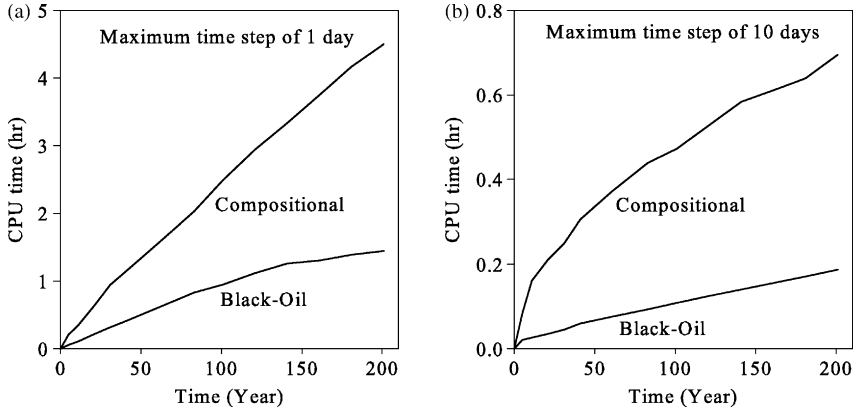

Fig. 6 – Black-oil and compositional simulators CPU time for two maximum allowable time steps of 1 (a) and 10 (b) days presented as a function of CO_2 injection time.

simulation time-steps remained constant and equal to the maximum time-step with the exception of the injection period for both simulators. In the second case (maximum time step of 10 days), the black-oil simulator used the maximum allowable time-step (of 10 days) for most of the simulation time, but the compositional simulator used significantly smaller time-steps. Results presented in Fig. 6 reveal that the black-oil simulator performs three to four times faster than the compositional simulator for the simple problem studied in this work. As mentioned in the first case (maximum time step of 1 day), both simulators used the same number of time steps. Results demonstrate that the work per time step for the compositional approach is four times larger than that of black-oil simulation approach in this simple case.

While the black-oil simulator is able to use larger time steps, the compositional simulator is not able to use such large time step. When we relaxed the maximum time step for the black-oil simulator, a larger speed up factor was obtained. Furthermore, it was found that the compositional simulator is very sensitive to the time-step during well shut-in and opening. It is expected that for more difficult problems where a large number of wells are in operation, the black-oil simulator will demonstrate much faster simulations than the compositional model.

7. Discussion

This paper proposes the use of black-oil models for simulation studies of CO_2 storage in deep aquifers, and presents a simple and efficient algorithm for computing the necessary PVT data. For this purpose, the gaseous phase in the black-oil formulation was used to represent the super-critical CO_2 phase. This is appropriate for most scenarios of geological storage of CO_2, where the aquifer depth is more than 800–1000 m and the pressure and temperature conditions are above the CO_2 critical point. However, if conditions occur such that the CO_2 crosses a phase boundary leading to formation of a new phase, or the CO_2 is at near critical conditions where some of the thermodynamic models used in this study would be inaccurate, use of the black-oil simulation approach and/or the algorithms suggested in this paper would be inappropriate. Among other cases, such conditions may occur if the CO_2 travels to shallow depths as a result of leakage from the aquifer.

8. Summary and conclusions

Flow modeling of CO_2 sequestration in saline aquifers has been treated in the literature since the early 1990s. Accurate evaluation of capacity of a saline aquifer to sequester CO_2 by solubility trapping needs precise representation of PVT data for the CO_2–brine system. Compositional reservoir simulators that account for complex phase behavior and very compositionally dependent systems are computationally expensive compared to traditional black-oil simulators. Although such compositional models are well suited for enhanced oil recovery processes, like miscible gas injection, a CO_2–brine system allows a black-oil treatment. Simulation of large-scale, long-term geological storage of CO_2 is computationally intensive. However, by using a black-oil simulation approach, the computational burden of flow simulation can be reduced significantly. Equilibrium compositional data for a CO_2–brine system can be converted into traditional black-oil PVT data to account for CO_2 and water phase partitioning. Such an approach, indeed, has been used previously in the petroleum engineering literature for translating compositional information into a black-oil data for petroleum reservoir simulation (Kazemi et al., 1978; Aziz and Settari, 1979). In this paper, a new fluid module was developed based on a simple algorithm that allows generating black-oil PVT data required for flow modeling of CO_2 storage in saline aquifers. The fluid module was then validated with the experimental data available in the literature. It was shown that the proposed fluid module is able to provide fast and accurate representation of all the PVT input data required for the black-oil flow simulation of CO_2 storage in saline aquifers. Numerical simulations for a simple CO_2 storage case reveal that the black-oil simulation is at least four times faster than the compositional simulation. It is anticipated that the speed-up factor is much larger for more difficult problems. The accuracy in prediction of CO_2–brine black-oil PVT properties and improved computational efficiency increase confidence in application of black-oil simulation approach for field-scale geological storage of CO_2 in deep saline aquifers.

Acknowledgements

The authors would like to thank Nicolas Spycher for his review and constructive comments. Useful comments from the journal associate editor Stefan Bachu and two anonymous reviewers that improved the original version of the paper are acknowledged. The financial support for this work was provided by the National Science and Engineering Research Council of Canada (NSERC) and the Alberta Department of Energy. This support is gratefully acknowledged. The first author also thanks the National Iranian Oil Company (NIOC) for financial support.

Appendix A

The Redlich and Kwong EOS (1949) is given by

$$p = \frac{RT}{V - b_m} - \frac{a_m}{T^{0.5} V(V + b_m)} \tag{A1}$$

where V is the molar volume of the CO_2-rich phase; p pressure; T temperature; R gas constant; parameters a and b characterize intermolecular attraction and repulsion, respectively. Conventionally, a and b are obtained based on the critical properties of the components. The following CO_2 and water interaction parameters are used in the proposed module after Spycher et al. (2003): $a_{CO_2} = 7.54 \times 10^7 - 4.13 \times 10^4 T$ (bar cm^6 K$^{0.5}$ mol^{-2}) and $b_{CO_2} = 27.8$(cm^3/mol); $a_{H_2O-CO_2} = 7.89 \times 10^7$ (bar cm^6 K$^{0.5}$ mol^{-2}) and $b_{H_2O} = 18.18$ (cm^3/mol).

The mixture constants a and b are calculated using Prausnitz et al. (1986) mixing rules:

$$a_m = \sum_{i=1}^{N}\sum_{i=1}^{N} y_i y_j a_{ij} \tag{A2}$$

$$b_m = \sum_{i=1}^{N} y_j b_i \tag{A3}$$

The fugacity coefficient φ_k of a component can be obtained by the Prausnitz et al. (1986) formulation as

$$\ln\varphi_k = \ln\left(\frac{V}{V-b_m}\right) + \left(\frac{b_k}{V-b_m}\right) - \left(\frac{2\sum_{i=1}^{N} y_i a_{ik}}{RT^{1.5}b_m}\right)\ln\left(\frac{V+b_m}{V}\right) + \left(\frac{a_m b_k}{RT^{1.5}b_m^2}\right)\left[\ln\left(\frac{V+b_k}{V}\right) - \left(\frac{b_m}{V+b_m}\right)\right] - \ln\left(\frac{PV}{RT}\right) \tag{A4}$$

The volume of the gas can be calculated from the following cubic equation:

$$V^3 - V^2\left(\frac{RT}{p}\right) - V\left(\frac{RTb_m}{p} - \frac{a_m}{pT^{0.5}} + b_m^2\right) - \left(\frac{a_m b_m}{pT^{0.5}}\right) = 0 \tag{A5}$$

where $R = 83.1447$ bar cm^3 mol^{-1} K^{-1}; V is in cm^3/mol; p is in bar; T is in K; b is in cm^3/mol; a is in bar cm^6 K$^{0.5}$ mol^{-2}.

Appendix B. Procedure for converting compositional phase equilibrium data into black-oil PVT data

(1) Calculate gas molar volume by Eq. (A5).
(2) Calculate gas compressibility factor by PV/RT.
(3) Calculate fugacity coefficient for each component by using Eq. (A4).
(4) Calculate CO_2 molality in pure water ($m^0_{CO_2}$) as outlined below:

$$y_{H_2O} = \frac{1-B}{1/A-B} \tag{B1}$$

where

$$B = \frac{\varphi_{CO_2} p}{55.508\kappa^0_{CO_2(g)}}\exp\left[-\frac{(p-p^0)\bar{V}_{CO_2}}{RT}\right] \tag{B2}$$

$$A = \frac{\kappa^0_{H_2O(g)}}{\varphi_{H_2O} p}\exp\left[\frac{(p-p^0)\bar{V}_{H_2O}}{RT}\right] \tag{B3}$$

$$x_{CO_2} = B(1-y_{H_2O}) \tag{B4}$$

$$m^0_{CO_2} = \frac{55.508 x_{CO_2}}{x_{H_2O}} \tag{B5}$$

(5) Calculate CO_2 molality in pure water (m_{CO_2}) as outlined below:

First use Eq. (12) to calculate γ^* then calculate $m_{CO_2} = m^0_{CO_2}/\gamma^*$.

(6) Calculate water and CO_2 mole fractions and equilibrium ratios using Eqs. (14)–(19).
(7) Calculate brine density and compressibility using Rowe and Chou correlation (1970).

$$a_1 = 5.916365 - 0.01035794T + 0.9270048\times10^{-5}T^2 - \frac{1127.522}{T} + \frac{100674.1}{T^2} \tag{B6}$$

$$a_2 = 0.520491\times10^{-2} - 0.10482101\times10^{-4}T + 0.8328532\times10^{-8}T^2 - \frac{1.1702939}{T} + \frac{102.2783}{T^2} \tag{B7}$$

$$a_3 = 0.118547\times10^{-7} - 0.6599143\times10^{-10}T \tag{B8}$$

$$a_4 = -2.5166 + 0.0111766T - 0.170522\times10^{-4}T^2 \tag{B9}$$

$$a_5 = 2.84851 - 0.0154305T + 0.223982\times10^{-4}T^2 \tag{B10}$$

$$a_6 = -0.0014814 + 0.829639\times10^{-5}T - 0.12469\times10^{-7}T^2 \tag{B11}$$

$$a_7 = 0.0027141 - 0.15391\times10^{-4}T + 0.22655\times10^{-7}T^2 \tag{B12}$$

$$a_8 = 0.62158\times10^{-6} - 0.40075\times10^{-8}T + 0.65972\times10^{-11}T^2 \tag{B13}$$

$$\frac{1}{\rho} = (a_1 - \pi a_2 - \pi^2 a_3 + a_4 S + a_5 S^2 - \pi a_6 S - \pi a_7 S^2 - 0.5\pi^2 a_8 S)\times10^{-3} \tag{B14}$$

$$c_b(p) = \frac{\rho_p - \rho_r}{\rho_p(p-p_r)} \tag{B15}$$

where c_b is in kPa^{-1}; T is in K; π is pressure in kgf/cm^2; ρ is in kg/m^3 at pressure p; S is salt mass fraction; p is pressure in kPa; ρ_r is brine density in kg/m^3 at reference pressure (p_r = 101.325 kPa).

(8) Calculate the aqueous phase (CO_2 saturated) density by Eq. (20) (Garcia, 2001).
(9) Calculate solution gas–oil ratio and water formation volume factor by Eqs. (24) and (25), respectively.

Appendix C. Correlations for transport properties of CO_2 and brine

C.1. Brine viscosity

Kestin et al. (1981) presented a correlation for aqueous NaCl solution viscosity as a function of temperature, pressure, and brine salinity. The effect of dissolved CO_2 may be ignored as proposed by Sayegh and Najman (1987), Enick and Klara (1992), and Batzle and Wang (1992). Their viscosity correlation takes the following form:

$$\mu_b = \mu^0(\theta, m) + \left[1 + \frac{\pi}{10^9}\sum_{i=0}^{4}\beta_i m^i\right] \tag{C1}$$

Table C1 – Various constants needed for calculation of CO_2 and brine viscosities

Constant	0	1	2	3	4	5
a_i		3.324×10^{-2}	3.624×10^{-2}	-1.879×10^{-4}		
b_i		-3.96×10^{-2}	1.02×10^{-2}	7.02×10^{-4}		
c_i		1.2378	-1.303×10^{-3}	3.06×10^{-6}	2.55×10^{-8}	
d_i		6.044	2.8×10^{-3}	3.6×10^{-5}		
e_i	0.235156	−0.491266	5.211155×10^{-2}	5.347906×10^{-2}	-1.537102×10^{-2}	
f_i		5.5934×10^{-3}	6.1757×10^{-5}	0.0	2.6430×10^{-11}	
g_i		0.4071119×10^{-2}	0.7198037×10^{-4}	$0.2411697 \times 10^{-16}$	0.297107×10^{-22}	$-0.1627880 \times 10^{-22}$
β_I	−1.297	5.74×10^{-2}	-6.97×10^{-4}	4.47×10^{-6}	-1.05×10^{-8}	
β_i^*		2.5	−2.0	0.5		

where

$$\log\left(\frac{\mu^0(\theta,m)}{\mu_w^0(\theta)}\right) = \sum_{i=1}^{3} a_i m^i + \sum_{i=1}^{3} b_i m^i \left\{\frac{1}{96+\theta}\sum_{i=1}^{4} c_i(\theta-20)\right\} \quad \text{(C2)}$$

$$\beta(T,m) = \left\{0.545 + 2.8\times10^{-3} - \sum_{i=0}^{4}\beta_i m^i\right\}\left\{\sum_{i=1}^{3}\beta_i^*\left(\frac{m}{m_s}\right)\right\} + \sum_{i=0}^{4}\beta_i m^i \quad \text{(C3)}$$

$$m_s = \sum_{i=0}^{2} d_i T^i \quad \text{(C4)}$$

μ_b is in μPa s, θ is in °C, π is in Pa, m is salt molality, and μ_w^0 (20 °C) = 1002.0 μPa s.

Various constants in the above equations are given in Table C1.

C.2. Gas phase viscosity

To calculate viscosity of the gas phase, traditional black-oil assume that the gaseous phase is pure CO_2. Vesovic et al. (1990) and Fenghour et al. (1998) presented correlations to calculate CO_2 viscosity under a wide range of pressures and temperatures as given below.

$$\mu(\rho,T) = \frac{1.00697T^{1/2}}{\psi_\mu^*(T^*)} + g_1\rho + g_2\rho^2 + \frac{g_3\rho^6}{T^{*3}} + g_4\rho^8 + \frac{g_5\rho^8}{T^*} + \sum_{i=1}^{4} f_i\rho \quad \text{(C5)}$$

where $T^* = kT/\varepsilon$ and ε/k = 251.196 K, ρ is in kg/m^3, T is in K, μ is in μPa s and

$$\ln\psi_\mu^*(T^*) = \sum_{i=0}^{4} e_i(\ln T^*)^i \quad \text{(C6)}$$

Various constants in the above equations are given in Table C1.

C.3. Molecular diffusion coefficient

At constant temperature, the diffusion coefficient of CO_2 into brine can be determined with the diffusion coefficient of CO_2 into water according to the following (Ratcliff and Holdcroft, 1963; Al-Rawajfeh, 2004):

$$\log\left(\frac{D_0}{D_b}\right) = 0.87\log\left(\frac{\mu_b}{\mu_0}\right) \quad \text{(C7)}$$

where D_0 and μ_0 denote the molecular diffusion of CO_2 in water and water viscosity, respectively. The diffusion coefficient of CO_2 in pure water is calculated by the following correlation (McLachlan and Danckwerts, 1972):

$$\log D_0 = -4.1764 + \frac{712.52}{T} - \frac{2.5907\times10^5}{T^2} \quad \text{(C8)}$$

where D is in m^2/s and T is in Kelvin.

REFERENCES

Adams, J.J., Bachu, S., 2002. Equations of state for basin geofluids: algorithm review and intercomparison for brines. Geofluids 2, 257–271 Erratum: Geofluids (2004) 4, 250.

Al-Rawajfeh, A.E., 2004. Modelling and simulation of CO_2 release in multiple-effect distillers for seawater desalination. Ph.D. Dissertation, Martin-Luther University of Halle-Wittenberg. Department of Engineering Sciences, Institute of Thermal Process Engineering, Halle (Saale), Germany, pp. 8–10.

Amyx, J.W., Bass Jr., D.M., Whiting, R.L., 1960. Petroleum Reservoir Engineering—Physical Properties. McGraw-Hill, New York.

Aziz, K., Settari, A., 1979. Petroleum Reservoir Simulation. Elsevier Applied Science Publishers, London.

Bachu, S., Adams, J.J., 2003. Estimating CO_2 sequestration capacity in solution in deep saline aquifers. Energy Conv. Manage. 44 (20), 3151–3175.

Bamberger, A., Sieder, G., Maurer, G., 2000. High-pressure (vapour + liquid) equilibrium in binary mixtures of (carbon dioxide + water or acetic acid) at temperatures from 313 to 353 K. J. Supercrit. Fluids 17, 97–100.

Battistelli, A., Calore, C., Pruess, K., 1997. The simulator TOUGH2/EWASG for modeling geothermal reservoirs with brines and non-condensable gas. Geothermics 26, 437–464.

Batzle, M., Wang, Z., 1992. Seismic properties of pore fluids. Geophysics 57, 1396–1408.

Blair, L.M., Quinn, J.A., 1968. Measurement of small density differences: solubility of slightly soluble gases. Rev. Sci. Instrum. 39 (1), 75–77.

Briones, J.A., Mullins, J.C., Thies, M.C., 1987. Ternary phase equilibria for acetic acid–water mixtures with supercritical carbon dioxide. Fluid Phase Equilib. 36, 235–246.

Chang, Y.B., Coats, B.K., Nolen, J.S., 1998. A compositional model for CO_2 floods including CO_2 solubility in water. SPE Reser. Evaluat. Eng. 1 (2), 155–160.

Craft, B.C., Hawkins, M., Terry, R.E., 1991. Applied Petroleum Reservoir Engineering, 2nd ed. Prentice Hall, Englewood Cliffs, New Jersey.

Diamond, L., Akinfiev, N., 2003. Solubility of CO_2 in water from −1.5 to 100 °C and from 0.1 to 100 MPa: evaluation of literature data and thermodynamic modelling. Fluid Phase Equilib. 208, 265–290.

Dodds, W.S., Stutzman, L.F., Sollami, B.J., 1956. Carbon dioxide solubility in water. Ind. Eng. Chem., Chem. Eng. Data Ser. 1, 92–95.

Dohrn, R., Bünz, A.P., Devlieghere, F., Thelen, D., 1993. Experimental measurements of phase equilibria for ternary and quaternary systems of glucose, water, CO_2 and ethanol with a novel apparatus. Fluid Phase Equilib. 83, 149–158.

D'Souza, R., Patrick, J.R., Teja, A.S., 1988. High pressure phase equilibria in the carbon dioxide–*n*-hexadecane and carbon dioxide water systems. Can. J. Chem. Eng. 66, 319–323.

Duan, Z., Sun, R., 2003. An improved model calculating CO_2 solubility in pure water and aqueous NaCl solutions from 273 to 533 K and from 0 to 2000 bar. Chem. Geol. 193 (3–4), 257–271.

Duan, Z., Sun, R., Zhu, C., Chou, I.-M., 2006. An improved model for the calculation of CO_2 solubility in aqueous solutions containing Na^+, K^+, Ca^{2+}, Mg^{2+}, Cl^-, and SO_4^{2-}. Mar. Chem. 98 (2–4), 131–139.

Enick, R., Klara, S., 1990. CO_2 solubility in water and brine under reservoir conditions. Chem. Eng. Commun. 90, 23–33.

Enick, R.M., Klara, S.M., 1992. Effects of CO_2 solubility in brine on the compositional simulation of CO_2 floods. SPE Reser. Eng. J. 7 (2), 253–258.

Ennis-King, J., Paterson, L., 2003. Rate of dissolution due to convective mixing in the underground storage of carbon dioxide. In: Gale, J., Kaya, Y. (Eds.), Proceedings of the 6th International Conference on Greenhouse Gas Control Technologies 2002, 1. Elsevier, Kyoto, Japan, pp. 507–510.

Ennis-King, J., Paterson, L., 2005. Role of convective mixing in the long-term storage of carbon dioxide in deep saline formations. SPE J. 10 (3), 349–356.

Ennis-King, J.P., Preston, I., Paterson, L., 2005. Onset of convection in anisotropic porous media subject to a rapid change in boundary conditions. Phys. Fluids 17, 084107–84115.

Fenghour, W., Wakeham, A., Vesovic, V., 1998. The viscosity of carbon dioxide. J. Phys. Chem. Ref. Data 27 (1), 31–44.

Garcia, J.E., 2001. Density of aqueous solutions of CO_2. LBNL Report 49023, Lawrence Berkeley National Laboratory, Berkeley, CA.

GEM, Version, 2004. User Manual, Computer Modeling Group, Calgary, Canada.

Gillespie P.C., Wilson, G.M., 1982. Vapor–liquid and liquid–liquid equilibria: water–methane, water–carbon dioxide, water–hydrogen sulfide, water–*n*-pentane, water–methane–*n*-pentane. Research Report RR-48, Gas Processors Association, Tulsa, OK.

Hassanzadeh, H., 2006. Mathematical modeling of convective mixing in porous media for geological CO_2 storage. Ph.D. Dissertation, University of Calgary.

Hassanzadeh, H., Pooladi-Darvish, M., Keith, D., 2005. Modeling of convective mixing in CO_2 storage. J. Can. Pet. Technol. 44 (10), 43–51.

Honarpour, M., Koederitz, L.F., Harvey, H.A., 1982. Empirical equations for estimating two-phase relative permeability in consolidated rock. J. Pet. Technol. 34, 2905–2908.

Hnedovsky, L., Wood, R.H., Majer, V., 1996. Volumes of aqueous solutions of CH_4, CO_2, H_2S, and NH_3 at temperatures from 298.15 K to 705 K and pressures to 35 MPa. J. Chem. Thermodyn. 28 (2), 125–142.

IMEX, Version 2004. User Manual, Computer Modeling Group, Calgary, Canada.

Kazemi, H., Vestal, C.R., Shank, G.D., 1978. An efficient multicomponent numerical simulator. Soc. Pet. Eng. J. Oct. 355–368.

Kestin, J., Khalifa, E., Correia, R.J., 1981. Tables of the dynamic and kinematic viscosity of aqueous NaCl solutions in the temperature range 20–150 °C and the pressure range 0.1–35 MPa. J. Phys. Chem. Ref. Data 10 (1), 71–87.

King, M.B., Mubarak, A., Kim, J.D., Bott, T.R., 1992. The mutual solubilities of water with supercritical and liquid carbon dioxide. J. Supercrit. Fluids 5, 296–302.

Lindeberg, E.G.B., Wessel-Berg, D., 1996. Vertical convection in an aquifer column under a gas cap of CO_2. Energy Conv. Manage. 38S, 229–234.

Malinin, S.D., Savelyeva, N.I., 1972. The solubility of CO_2 in NaCl and $CaCl_2$ solutions at 25, 50 and 75 °C under elevated CO_2 pressures. Geochem. Int. 9, 410–418.

Malinin, S.D., Kurovskaya, N.I., 1975. Solubility of CO_2 in chloride solutions at elevated temperatures and CO_2 pressures. Geochem. Int. 12, 199–201.

McLachlan, C.N.S., Danckwerts, P.V., 1972. Desorption of carbon dioxide from aqueous potash solutions with and without the addition of arsenite as a catalyst. Trans. Inst. Chem. Eng. 50, 300–309.

Müller, G., Bender, E., Maurer, G., 1988. das dampf-flüssigkeitsgleichgewicht des ternären systems ammoniak-kohlendioxid-Wasser bei hohen wassergehalten im bereich zwischen 373 und 473 Kelvin. Berichte der Bunsen-Gesellshaft für Physikalische Chemie 92, 148–160.

Pitzer, K.S., 1973. Thermodynamics of electrolytes. 1. Theoretical basis and general equations. J. Phys. Chem. 77, 268–277.

Portier, S., Rochelle, C., 2005. Modelling CO_2 solubility in pure water and NaCl-type waters from 0 to 300 °C and from 1 to 300 bar—application to the Utsira Formation at Sleipner. Chem. Geol. 217 (3–4), 187–199.

Prausnitz, J.M., Lichtenthaler, R.N., Gomes de Azevedo, E., 1986. Molecular Thermodynamics of Fluid-Phase equilibria, 2nd ed. Prentice Hall, New Jersey.

Ratcliff, G.A., Holdcroft, J.G., 1963. Diffusivities of gases in aqueous electrolyte solutions. Trans. Inst. Chem. Eng. 41, 315–319.

Redlich, O., Kwong, J.N.S., 1949. On the thermodynamics of solutions. V. An equation of state. Fugacities of gaseous solutions. Chem. Rev. 44, 233–244.

Rowe, A.M., Chou, J.C.S., 1970. Pressure–volume–temperature–concentration relation of aqueous NaCl solutions. J. Chem. Eng. Data 15, 61–66.

Sako, T., Sugeta, T., Nakazawa, N., Okubo, T., Sato, M., 1991. Phase equilibrium study of extraction and concentration of furfural produced in reactor using supercritical carbon dioxide. J. Chem. Eng. Jpn. 24 (4), 449–455.

Sayegh, S.G., Najman, J., 1987. Phase behaviour measurements of CO_2–SO_2–brine mixtures. Can. J. Chem. Eng. 65, 314–320.

Settari, A., 2001. Topics in Reservoir Simulation. TAURUS Reservoir Solutions Ltd., Calgary, Alta., Canada.

Song, K.Y., Kobayashi, R., 1987. Water content of CO_2 in equilibrium with liquid water and/or hydrates. SPE Form. Eval. 2, 500–508.

Span, R., Wagner, W., 1996. A new equation of state for carbon dioxide covering the fluid region from the triple-point temperature to 1100 K at pressures up to 800 MPa. J. Phys. Chem. Ref. Data 25 (6), 1509–1596.

Spycher, N., Pruess, K., 2005. CO_2–H_2O mixtures in the geological sequestration of CO_2. II. Partitioning in chloride brines at 12–100 °C and up to 600 bar. Geochim. Cosmochim. Acta 69 (13), 3309–3320.

Spycher, N., Pruess, K., Ennis-King, J., 2003. CO_2–H_2O mixtures in the geological sequestration of CO_2. I. Assessment and calculation of mutual solubilities from 12 to 100 °C and up to 600 bar. Geochim. Cosmochim. Acta 67 (16), 3015–3031.

Teng, H., Yamasaki, A., Chum, M.-K., Lee, H., 1997. Solubility of liquid CO_2 in water at temperatures from 278 K to 293 K and pressures from 6.44 MPa to 29.49 MPa and densities of the corresponding aqueous solutions. J. Chem. Thermodyn. 29, 1301–1310.

Tödheide, K., Frank, E.U., 1963. Das Zweiphasengebiet und die Kritische Kurve im System Kohlendioxid-Wasser bis zu Drucken von 3500 bar. Z. Phys. Chem., Neue Folge 37, 387–401.

Vesovic, V., Wakeham, W.A., Olchowy, W.A., Sengers, J.V., Watson, J.T.R., Millat, J., 1990. The transport properties of carbon dioxide. J. Phys. Chem. Ref. Data 19, 763–808.

Walsh, M., Lake, L.W., 2003. Generalized Approach to Primary Hydrocarbon Recovery. Elsevier, Amsterdam.

Wiebe, R., Gaddy, V.L., 1939. The Solubility in water in carbon dioxide at 50, 75, and 100 °C, at pressures to 700 atmospheres. J. Am. Chem. Soc. 61, 315–318.

Wiebe, R., Gaddy, V.L., 1940. The solubility of carbon dioxide in water at various temperatures from 12 to 40 and at pressures to 500 atmospheres. Critical phenomena. J. Am. Chem. Soc. 62, 815–817.

Wiebe, R., 1941. The binary system carbon dioxide–water under pressure. Chem. Rev. 21, 475–481.

Wong, C.S., Tishchenko, P.Ya., Johnson, W.K., 2005. Effects of high CO_2 molality on the carbon dioxide equilibrium of seawater. J. Chem. Eng. Data 50 (3), 822–831.